OBSERVATION OF EVENTS AT VERY HIGH Q^2 IN ep COLLISIONS AT HERA

E.PEREZ, on behalf of H1 Collaboration
CEA-Saclay, DSM/DAPNIA/SPP, Gif-sur-Yvette, France

Abstract

Deep-inelastic scattering events produced in positron-proton collisions with squared momentum transfers Q^2 up to 35000 GeV^2 has been studied at HERA.
For $Q^2 > 15000$ GeV^2, 12 neutral current candidate events are observed where the expectation of the standard deep-inelastic model of lepton-nucleon scattering is 4.71 ± 0.76 events. In the same Q^2 range, 4 charged current candidates are observed where the expectation is 1.77 ± 0.87 events. The difference in the observed and expected number of neutral current events is mostly due to events in which the positron is backscattered at large angles.

1 Introduction

The ep collider HERA is a unique facility for probing the proton at very small distances ($\simeq 10^{-16}$ cm) via t-channel exchange of a highly virtual gauge boson [1, 2, 3]. This resolution power is ten times higher than the one obtained at previous lepton-nucleon scattering experiments. HERA is also ideally suited to search for new particles possesing couplings to lepton-quark pairs, such as leptoquarks or squarks in R-parity violating supersymmetry, with masses up to the kinematic limit of $\sqrt{s} \simeq 300$ GeV. These could be produced in resonance via a fusion between the incident positron and a parton coming from the proton [4]. Measurements of Neutral Current (NC) and Charged Current (CC) Deep Inelastic Scattering (DIS) are considered here. This analysis relies on H1 e^+p data collected from 1994 to 1996, corresponding to an integrated luminosity of $\mathcal{L} = 14.19 \pm 0.32$ pb^{-1}, an increase of a factor five compared to above cited earlier studies. The positron beam energy was $E_e^0 = 27.55$ GeV, the proton beam energy was $E_p = 820$ GeV. All details concerning this analysis can be found in [5]. A similar study carried out by ZEUS Collaboration is described in [6].

2 Kinematics of Deep-inelastic scattering

The lowest order DIS process is represented in Fig. 1. The kinematics of DIS is described by two independent variables, which can be chosen among the three usual Lorentz invariants Q^2, x and y, related by $Q^2 = xyS$. Their definition is reminded on Fig. 1. Q^2 describes the

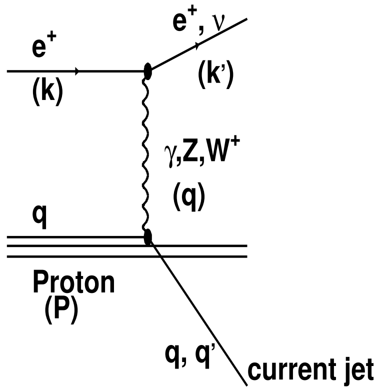

$$Q^2 = -q^2 = -(k - k')^2$$

$$x = \frac{Q^2}{2(P.q)}$$

$$y = \frac{(P.q)}{(P.k)} = \frac{1+\cos\theta_e^*}{2}$$

Figure 1: Lowest order DIS diagram and definition of usual Lorentz invariants.

virtuality of the exchanged boson. In the parton model, x corresponds to the fraction of the proton momentum carried by the interacting quark. Instead of using x, we can equivalently define $M = \sqrt{xS}$, which is the invariant mass in the eq CM frame. The variable y is also related to the polar angle[1] θ_e^* of the scattered positron in this eq CM frame.

The kinematics of DIS scattering being overconstrained, several methods can be used to reconstruct Q^2, M and y :

- the **e-method** uses only information on the scattered positron, namely its energy and polar angle. The resolution on M degrades for the lowest values of y as $\delta M_e/M_e \propto 1/y_e$;

[1] The z axis is taken to be in the direction of the incident proton.

- the 2α**-method** uses the polar angles of both the scattered positron and the hadronic final state;
- the **h-method** (or Jacquet-Blondel method) uses the full information on the hadronic flow, and is of course the only available method to reconstruct kinematics of charged current events. Resolutions on both M_h and Q_h^2 degrade for the highest values of y as $1/1 - y_h$.

Detailed formulae for each reconstruction method can be found in [5]. The 2α-method is insensitive to the absolute calibration, unlike the e-method. But, in case of QED initial state radiation on the positron line, the estimatations of M with the 2α-method suffer from important shifts towards higher values. This can be seen in Fig 2, when a photon is emitted from the inital state positron, carrying a fraction $z = 10\%$ of its momentum. Fig. 2 also shows that

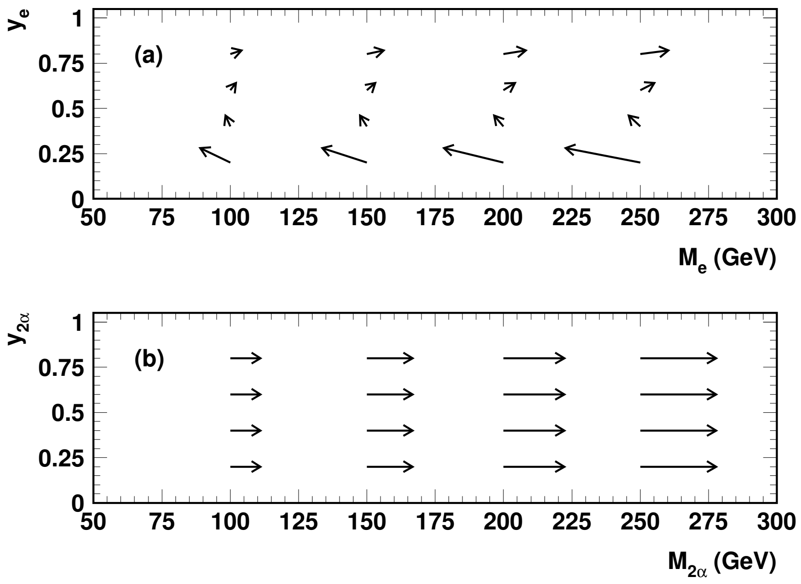

Figure 2: Influence of initial state radiation on the reconstruction of M and y, for (a) the e-method and (b) the 2α-method. The start points of the arrows indicate the true values of M and y, the end points the reconstructed values assuming that a photon carrying 10% of the initial state positron momentum has been emitted.

ISR leads to shifts on M_e towards lower values for $y < 0.5$, and towards higher values for high y. However, M_e is not dramatically overestimated for high y.
The analysis presented here relies on the e-method, the 2α-method being used as a cross-check.

3 Event selection

The full selection requirements applied in this analysis can be found in [5]. A first set of cuts are applied in order to ensure that the selected event sample is free of background not related to e^+p collisions, such as beam gas, beam halo or cosmic muon events.

3.1 Neutral Current selection

In order to select NC DIS events in the high Q^2 domain, the cuts mainly rely on calorimetric information :

1. an isolated positron[2] has to be found in the Liquid Argon calorimeter, in the polar angular range $10^\circ < \theta_e < 145^\circ$ and with a transverse energy $E_{T,e} > 25$ GeV; there must be at least one charged track within the positron isolation cone of opening $\delta R = \sqrt{(\delta\eta_e)^2 + (\delta\Phi_e)^2} = 0.25$, where the pseudorapidity η_e is defined as $\eta_e = -\ln\tan\theta_e/2$;
2. a total transverse momentum balance $P_{T,miss}/\sqrt{E_{T,e}} < 3\sqrt{\text{GeV}}$;
3. a limited momentum loss in the positron beam direction, $43 \leq \sum(E - P_z) \leq 63$ GeV;

Cut (2) takes into account the natural scale of the hadronic energy resolution. By energy-momentum conservation, the $\sum(E - P_z)$ distribution for NC DIS events is peaked at $2E_e^0$. This fact is exploited by cut (3), which rejects events where a very hard collinear γ is emitted by the initial state positron. The analysis is restricted to the kinematic domain $Q_e^2 > 2500$ GeV^2 and $0.1 < y_e < 0.9$. The low y_e domain, where M_e is badly measured (see section 2), is exluded. Excluding the high y_e values avoids the region where QED ISR effects are important, and also suppresses the photoproduction background (see section 5).

3.2 Charged current selection

Charged current DIS candidates are selected by applying the following requirements :

1. a total missing transverse momentum $P_{T,miss} = P_{T,h} > 50$ GeV;
2. a matching between the scalar and vectorial transverse energies $(E_T - P_{T,h})/E_T < 0.5$;

The analysis is restricted to the domain $y_h < 0.9$, which avoids the region where both M_h and Q_h^2 are badly reconstructed. Together with cut (1), this ensures that the selected events are in the range $Q_h^2 > 2500$ GeV^2.

4 Standard Model of Deep-Inelastic Scattering

To calculate an expectation for DIS ep scattering, we rely on the parton model in the approximation of single γ/Z and W boson exchange. Detailed expressions for the cross-sections which contain a description of the proton in terms of scale dependent structure functions can be found in [3]. For NC DIS, the contribution of the longitudinal structure function F_L is neglected. The structure functions are expressed in terms of parton densities which are taken here from the Martin-Roberts-Stirling MRS (H) [7] parametrizations. These were determined by a global fit of structure functions measurements in fixed target experiments (BCDMS,NMC,CCFR,EMC), inclusive lepton production and direct photon production (CDF, WA70,E605,UA6), and low Q^2 structure functions measurements at HERA [8, 9]. The next-to-leading order DGLAP [10] equations are used to evolve the parton densities to the high Q^2 relevant for this analysis. For the comparison with data, a Monte-Carlo simulation using the event generator DJANGO [11] has been performed, followed by a full simulation of the

[2] The analysis does not distinguish explicitly between e^- and e^+, i.e. no charge criteria is applied in order to select a positron candidate.

response of the H1 detector. The simulated samples for NC and CC DIS processes amount to about 100 times the integrated luminosity of the data.
The total systematic uncertainty has both experimental and theoretical sources. Experimental errors come from uncertainties on the integrated luminosity of $\pm 2.3\%$, and on the absolute electromagnetic (resp. hadronic) energy scale of $\pm 3\%$ (resp. $\pm 4\%$). In addition, a 7% theoretical uncertainty on the predicted cross-sections originates from the uncertainties on the parton density distributions of $\pm 5\%$, on the value of the strong coupling constant α_s of $\pm 4\%$, and on higher order QED corrections, of $\pm 2\%$ in the y range considered here.

All analyses described in the following sections have been repeated with an independent shift of the central values by ± 1 standard deviation of each of the experimental and theoretical sources of errors. The overall systematic error of the standard DIS model prediction is determined as the quadratic sum of the resulting errors and of the statistical error on the Monte Carlo simulation.

5 Background sources

The contributions from background processes which could give rise to events with true or misidentified isolated positrons at high E_T or to events with a large $P_{T,miss}$ were evaluated using the full simulation and reconstruction program chain. The background processes considered comprise photoproduction at large E_T, single production of real W and Z bosons, heavy flavour production, prompt photon production and two-photon processes. In order to ensure that the background contamination is negligible, specific cuts are added to the selection requirements described in section 3. These additionnal cuts lead to a 5% efficiency loss for DIS events. Applying all selection cuts and background rejection cuts leads to a remaining background contamination which is below 0.1% at 95% confidence level for the NC DIS sample. Hence, the background is negligible when compared to the estimated errors on the standard NC DIS expectation. This statement is also valid in a restricted kinematic range of $Q^2 > 10000$ GeV^2 where less than 0.1 (95% CL) background events are expected. Moreover, the purity of both NC and CC selected samples was cross-checked by relaxing the selection cuts and by visual scan of the events.

6 Analysis

We observe 443 NC DIS candidates satisfying all the selection criteria, which is in good agreement with the expectation of 427 ± 38 from NC DIS processes. Within the kinematic range considered, the ratio of this expected number of events to the number generated by the Monte Carlo simulation is about 80% due to experimental acceptance and event selection.
For the CC DIS candidates, 31 events are found satisfying the above requirements, which agrees well with the expectation of 34.2 ± 5.8 from CC DIS processes. Here the corresponding ratio of accepted to generated events is again about 80% in the $P_{T,miss}$ and y_h range considered.

Fig. 3 shows the two dimensional distribution of y_e against M_e for the 443 events of our NC sample. For these 443 events, the distributions of the energy and polar angle of the scattered positron, and of the missing transverse momentum, are well reproduced by the NC DIS simulation, except for the largest values of the positron energy E_e. This will be

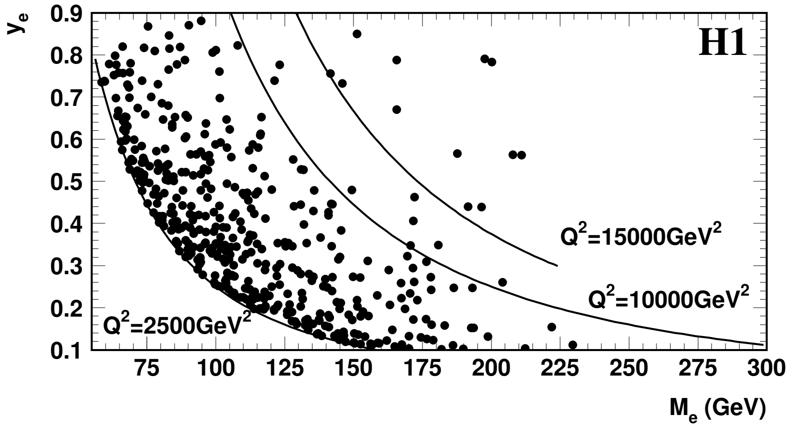

Figure 3: Selected NC DIS candidate events in the M_e - y_e plane; three contours of fixed Q^2 are also shown.

quantified below in terms of Q^2, to which E_e is closely related at large values.

6.1 Q^2 dependence

The measured Q_e^2 distribution is compared with expectation from NC DIS processes in Fig. 4a. The ratio of the measured Q_e^2 distribution to the NC DIS expectation is shown in Fig. 4b, together with the 1σ error contours. The total error on this expectation is dominated by the uncertainty in the electromagnetic energy scale of the calorimeter. It varies between 8.5% at low Q_e^2 and 30% at the highest values of Q_e^2.
The NC DIS expectation agrees well with the data for $Q_e^2 \lesssim 15000$ GeV^2, while at larger Q_e^2 the number of events is in excess of the NC DIS expectation. For $Q^2 > 15000$ GeV^2, $N_{obs} = 12$ events are observed while 4.71 ± 0.76 events are expected from NC DIS processes. The Poisson probability $\mathcal{P}(N \geq N_{obs})$ that in a random set of experiments the number of NC DIS events N in the range $Q_e^2 > 15000$ GeV^2 fluctuates to values equal to or larger than the observed number of events N_{obs}, taking into account the systematic uncertainty on the expectation, is calculated to be 0.6%.

For the charged current sample, both statistical and systematic uncertainties are larger. For $Q_h^2 > 15000$ GeV^2, 4 events are observed, while 1.77 ± 0.87 events are expected from standard CC DIS.

6.2 M_e and y_e dependence

The projected M_e and y_e distributions of the NC selected events in the "low" Q_e^2 range ($Q_e^2 < 15000$ GeV^2) are shown in Fig. 5a and 5b. These are well reproduced by the standard NC DIS expectation. The same comparison of data with expectation is performed in the "high" Q_e^2 domain ($Q_e^2 > 15000$ GeV^2) in Fig. 5c and 5d. It can be seen that the observed excess at high Q^2 is mainly concentrated at high values of M_e ($M_e \simeq 200$ GeV) and is most prominent at large y_e. Fig. 5e and 5f show the y_e distributions of the selected events in the "low" mass domain (100 GeV $< M_e < 180$ GeV) and in the high M_e domain ($M_e > 180$ GeV) respectively. Again, a difference appears between data and expectation at large masses and large y_e.

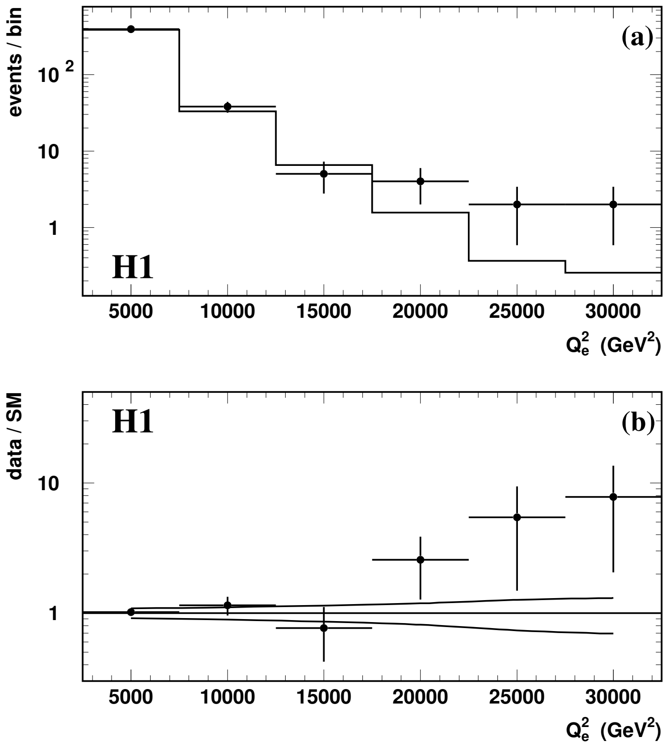

Figure 4: (a) Q_e^2 distribution of the selected NC DIS candidate events for the data (• symbols) and for standard NC DIS expectation (histogram); (b) ratio of the observed and expected number of events as a function of Q_e^2; the lines above and below unity specify the $\pm 1\sigma$ levels determined using the combination of statistical and systematic errors of the NC DIS expectation.

6.3 M_e dependence as a function of y_e

The measured and expected M_e distribution for two lower y_e cutoffs $y_{min} = 0.2$ and 0.4 are shown in Fig. 6a and 6c. The expectation well reproduces the data in the low masses domain, but an excess of events over the NC DIS expectation is seen at high M_e. At $M_e \simeq 200$ GeV, the data are several standard deviations above the expectation, as can be seen in Fig 6b and 6d. This difference becomes more visible with the larger y_{min} cut. For $M_e > 180$ GeV and $y_e > 0.4$, 7 events are observed in the data while 1.83 ± 0.33 are expected from NC DIS. This corresponds to a Poisson probability that the standard NC DIS signal fluctuates to values equal to or larger than the number of observed events of 3.8×10^{-3}. For $y_e > 0.4$ and in the mass intervall $M_e = 200 \pm 12.5$ GeV, the same 7 events are observed while 0.95 ± 0.18 events are expected, leading to a Poisson probability of 2.6×10^{-4} (this latter probability is in fact averaged over 3 steps of 1 GeV, when varying the central value of mass windows of width $\delta M_e = \pm 12.5$ GeV, as explained in [5]). The likeliness that, in a random set of experiments, such a fluctuation is observed *anywhere* in the mass range from 80 to 250 GeV is found to be less than 1%.

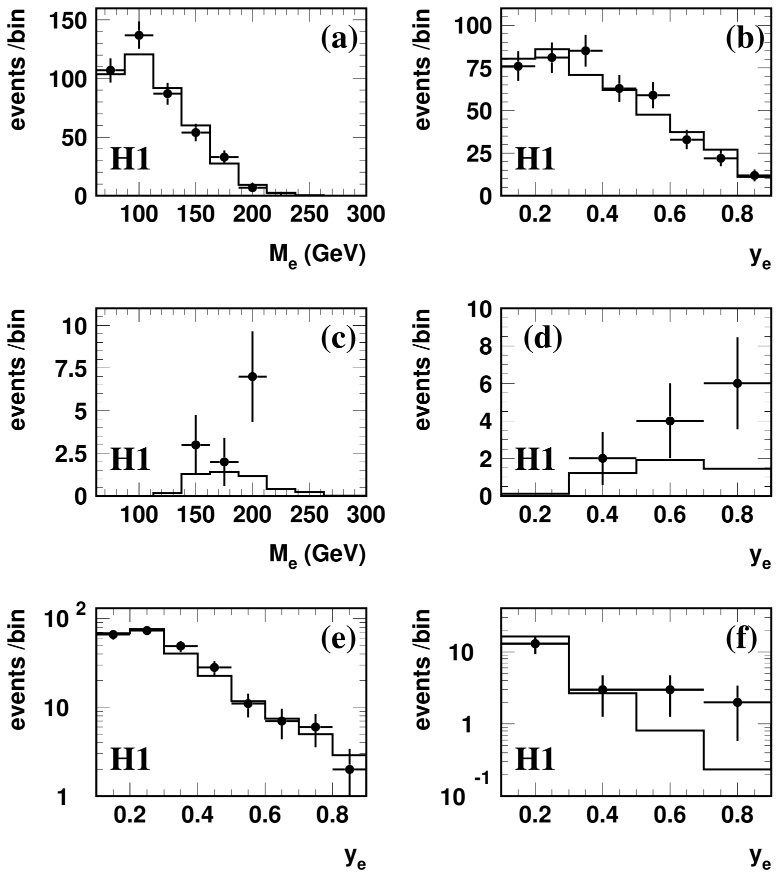

Figure 5: Distributions of M_e and y_e for selected NC DIS candidate events, (a) and (b) for $2500\,\mathrm{GeV}^2 < Q_e^2 < 15000\,\mathrm{GeV}^2$, (c) and (d) for $Q_e^2 > 15000\,\mathrm{GeV}^2$; distribution of y_e (e) for $100 < M_e < 180\,\mathrm{GeV}$ and (f) for $M_e > 180\,\mathrm{GeV}$; superimposed on the data points (• symbols) are histograms of the expectation of standard NC DIS.

6.4 The events at very high Q_e^2, M_e and y_e

The detailed kinematics of the 7 events observed at $M_e > 180$ GeV and $y_e > 0.4$ is given in Tab. 1. There is a good agreement between the different reconstruction methods, which gives evidence for the reliable reconstruction of the kinematics of these events. In particular, the two estimators M_e and $M_{2\alpha}$ are seen to agree well with each other and also with the invariant mass M_{e+jet} calculated from the positron and the highest E_T jet in the final state.

7 Non-standard contributions at high Q^2

7.1 New contributions in the standard DIS model

Varying the parton distribution functions, assuming different values for α_s, modifying the hadronisation model, allowing $F_L \neq 0$, does not lead to an enhancement of the cross-section at high Q^2 exceeding 20% of the standard value. Within the standard DIS model the only explanation of our result is therefore a statistical fluctuation.

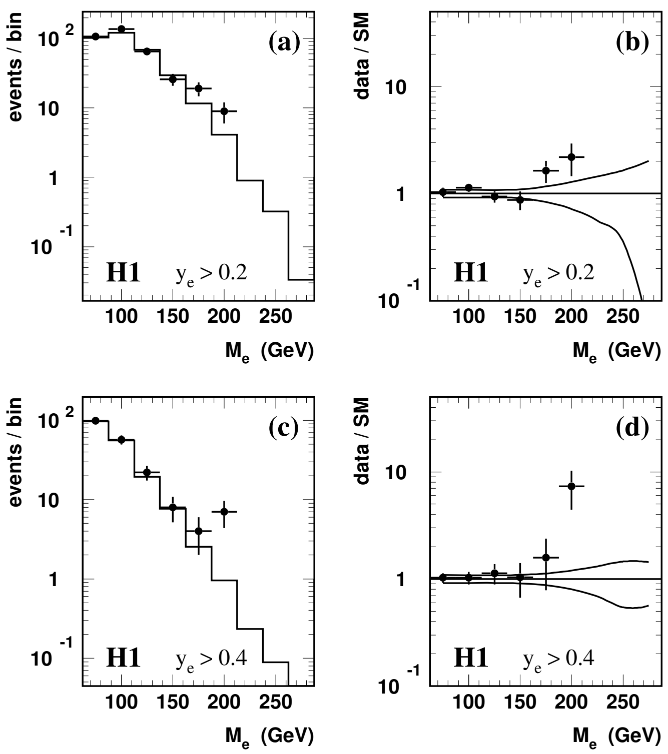

Figure 6: (a) Distribution of M_e for the observed (• symbols) NC DIS candidates with $y_e > 0.2$; the expectation from standard NC DIS is shown as the superimposed histogram; (b) ratio of the observed and expected numbers of events as a function of M_e for $y_e > 0.2$; (c) as in (a) but now with $y_e > 0.4$; (d) as in (b) but now with $y_e > 0.4$.

7.2 Physics Beyond the Standard Model

Beyond the Standard Model, the excess at high Q^2 and/or high M and y could be explained by different mechanisms. Leptoquarks, leptogluons or squarks in R-parity violating supersymmetry would be seen as narrow resonances in the mass distribution, although QCD corrections lead to a significant broadening of this distribution. The virtual exchange of new particles between positrons and partons or possible substructure of fermions inducing contact interactions could just lead to an enhancement of the cross-section at high Q^2.

8 Summary

For $Q^2 > 15000$ GeV^2, an excess of neutral current deep-inelastic scattering (DIS) events has been observed. Given the existing experimental constraints on parton density distributions at high M and lower Q^2, and given the agreement of the resulting predictions for e^+p DIS which is here reported for $Q^2 < 15000$ GeV^2, there is little freedom for an enhancement of the cross-section at higher Q^2 within the standard DIS model. Within this model, the only explanation is therefore a statistical fluctuation. This excess appears in a corner of phase space where new physics is not yet completely excluded by other experiments. Wether it can be interpreted in terms of new physics however requires larger statistics.

	M_e (GeV)	$M_{2\alpha}$ (GeV)	M_{e+jet} (GeV)	y_e	$y_{2\alpha}$	Q_e^2 (GeV^2)	$Q_{2\alpha}^2$ (GeV^2)
1	196	198	195	.439	.434	16950	17100
2	208	200	213	.563	.582	24350	23320
3	188	185	184	.566	.573	19950	19640
4	198	199	197	.790	.787	30870	31320
5	211	227	211	.562	.526	25030	27100
6	192	190	215	.440	.443	16130	16050
7	200	213	210	.783	.762	31420	34450

Table 1: NC DIS candidates satisfying the kinematic requirement $M > 180$ GeV and $y > 0.4$ when M and y are calculated with either the e-method or the 2α-method.

References

[1] ZEUS Collaboration, M. Derrick et al., Z. Phys. C67 (1995) 81; H1 Collaboration, S. Aid et al., Phys. Lett. B353 (1995) 578; ZEUS Collaboration, M. Derrick et al., Z. Phys. C72 (1996) 47.

[2] H1 Collaboration, S. Aid et al., Z. Phys. C67 (1995) 565.

[3] H1 Collaboration, S. Aid et al., Phys. Lett. B379 (1996) 319.

[4] H1 Collaboration, I. Abt et al., Nucl. Phys. B396 (1993) 3; ZEUS Collaboration, M. Derrick et al., Phys. Lett. B306 (1993) 173; H1 Collaboration, T. Ahmed et al., Z. Phys. C64 (1994) 545; H1 Collaboration, S. Aid et al., Phys. Lett. B369 (1996) 173; H1 Collaboration, S. Aid et al., Z. Phys. C71 (1996) 211; ZEUS Collaboration, M. Derrick et al., DESY preprint 96-161 (August 1996) 31pp., to be published in Z. Phys. C.

[5] H1 Collaboration,C. Adloff et al., Z. Phys. C74 (1997) 191.

[6] B. Straub, on behalf of ZEUS Collaboration, these proceedings; ZEUS Collaboration, J. Breitweg et al., Z. Phys. C74 (1997) 207.

[7] A.D. Martin, R.G. Roberts and W.J. Stirling, Durham Univ. preprint DTP-93-86 and Rutherford Appleton Lab. preprint RAL-93-077 (October 1993) 16pp.; A. D. Martin, R. G. Roberts and W. J. Stirling, Proc. of the Workshop on Quantum Field Theoretical Aspects of High Energy Physics, ed. B. Geyser and E.M. Ilgenfritz (1993), p. 11;

[8] H1 Collaboration, I. Abt et al., Nucl. Phys. B407 (1993) 515.

[9] ZEUS Collaboration, M. Derrick et al., Phys. Lett. B316 (1993) 412.

[10] Yu. L. Dokshitzer, JETP 46 (1977) 641; V. N. Gribov and L. N. Lipatov, Sov. Journ. Nucl. Phys. 15 (1972) 78; G. Altarelli and G. Parisi, Nucl. Phys. B126 (1977) 298.

[11] DJANGO 6.2; G.A. Schuler and H. Spiesberger, Proc. of the Workshop Physics at HERA, W. Buchmüller and G. Ingelman (Editors), (October 1991, DESY-Hamburg) Vol. 3 p. 1419.